

T.U.F.F: The Utility of Live Tension Measurements for Scientific Ballooning and Flight Dynamics

Jeremy J. Kuznetsov¹, Jaxon Lee¹, Daniel Grammer¹, J. Oliver Villegas¹,
Owen Moran¹, Malcolm Maas¹, and Mary Bowden²
University of Maryland, College Park, MD, 20742, U.S.A.

Abstract

Scientific balloon launches, like those performed by the Maryland Space Grant Consortium Balloon Payload Program (BPP), allow researchers to launch payloads and efficiently conduct experiments at high altitudes. The BPP Tension Under Flight Forces payload (TUFF) team has developed a supplemental payload that measures flightline tension on balloon missions. In this paper, we present practical applications for the tension data acquired, including the determination of partner-payload drag, measurement of swinging oscillation frequency, and modeling of the atmosphere. Through data analysis in Python 3.9.7, the TUFF team has shown the potential to pinpoint the drag experienced by partner payloads that share a flight, observe swinging patterns in tension oscillations, and measure the altitude of wind shear through tension variance caused by payload swinging. Tension measurement payloads offer a simple and light way to measure these values; however, there are certain drawbacks like their sensitive setup and calibration, which are also discussed in this paper. Although measurements and insights from the TUFF payload have not yet been used to enhance balloon flights, tension payloads could refine several parts of the ballooning process. Drag data can improve pre-flight helium calculations, which will aid in achieving targeted ascent rates, while oscillation data can help understand payload swinging conditions. Knowing more about flight conditions on ascent or during a float may enhance the performance of attitude stabilization payloads or safeguard cut-down modules, which are often rated to a maximum tension. More precise data about wind shear altitudes will improve balloon ground-track predictions and live tracking and has the potential to determine the altitude of the jet stream. Tension measuring devices have not been academically explored in the context of atmospheric ballooning, so this paper also acts as an overview of the TUFF design and project history.

I. Introduction	1
II. Payload Overview and Resources	2
III. Drag	5
IV. Oscillations	7
V. Shear	8
VI. Challenges and Potential Improvements	10
VII. Applications	11
VIII. Conclusions	13
IX. References	13
X. Acknowledgements and Appendices	13

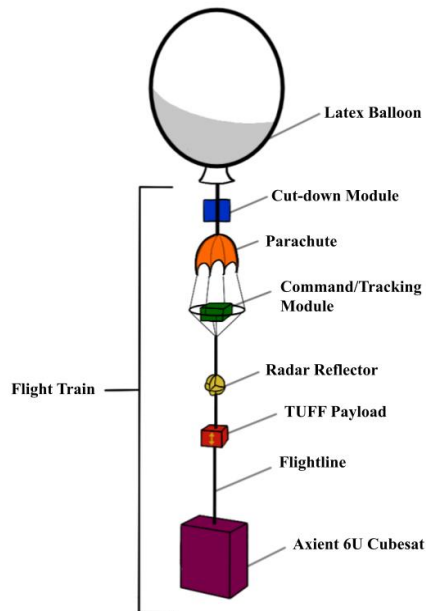
1. *Undergraduate Researcher at the University of Maryland, College Park*
2. *Senior Lecturer at the University of Maryland College Park, BPP Program Director*

I. Introduction

Upper-atmospheric ballooning has been an area of scientific interest for over a century. Today, many research teams, including the Maryland Space Grant Consortium Balloon Payload Program (BPP), conduct sounding balloon launches regularly. The research conducted on such high-altitude platforms ranges from atmospheric science data collection to the testing of low Earth orbit satellite systems. However, balloons are complicated to control, track, and operate precisely. Many uncertainties arise from the complex winds of the atmosphere and the involvement of partner payloads sharing a flight. The Tension Under Flight Forces device (TUFF) was developed by a team of researchers from BPP as a supplemental payload to help understand typical balloon and payload flight conditions. TUFF uses a strain-gauge load cell to measure the tension in a standard one-line flightline as pictured in *Figure 1*. This configuration allows for the simple and cheap integration of TUFF and similar systems on flights as long as safety precautions, discussed in *Section VI.B*, are taken.

Many details about payload flight dynamics are demonstrably useful for some ballooning payloads. Camera stabilization payloads, as an example, would benefit from information about how vigorously a payload line swings^{[1][3]}. Similarly, the altitude and intensity of wind shear is applicable to balloon ascent-rate and ground-track predictions. In turn, such knowledge regarding typical flight-paths is crucial for balloon tracking and live downlink capabilities, which may require close proximity to a balloon. Lastly, more details about payload drag can help to save helium while targeting precise ascent rates during the balloon inflation process.

In each of these cases, data acquired by TUFF may prove quite useful. Using the single measure of flightline tension, TUFF is potentially able to provide details about drag, oscillations in a flightline, and wind shear altitudes. This paper is an overview of the data collected and processed by the TUFF team in anticipation that our capabilities will prove useful to other ballooning teams. We have seen the potential to calculate the drag of specific partner payloads sharing a flight with TUFF, as well as the swinging caused by a flightline full of partner payloads. The strength of our evidence can be improved, as TUFF is a light and simple system that can be replicated and tested by others. Thus, any research team interested in TUFF's capabilities will find benefit in the overview of TUFF, its data, and its drawbacks. Specifically, data analysis of TUFF missions will be discussed in *Sections III, IV, and V*.



Finally, it is important to discuss the nomenclature that will be used throughout this paper. For common terms used by BPP to describe their flight configurations, refer to the labels in *Figure 1*. The most important distinction is that of the “Flight Train,” which describes an entire payload assembly carried by a given balloon, as opposed to the “Flightline,” which describes the continuous string that runs through each payload comprising the Flight Train. Although TUFF may be more accurately described as a measurement device, we will refer to it as a “payload” hereafter as per BPP nomenclature.

Note that the 6U test CubeSat was only included on TUFF's third flight. All other labeled components can be found on every TUFF flight, though the Radar Reflector and other payloads have been placed below TUFF in the past. The flight history of TUFF will be fully explained in *Section II*.

Fig 1. Standard Single-Line Flight Train Configuration.

II. Payload Overview and Resources

This section is predominantly for those interested in the history, construction, and operation procedures of the TUFF payload. To date, there have been two versions of the TUFF platform. The original version will hereafter be referred to as TUFF 1 while the succeeding version will be referred to as TUFF DOS, which denotes its specific missions of measuring drag, oscillations, and shear. Across the two versions of TUFF, there have been three flights.x

Flight Designation	Payload Model	Date	Duration of Total Flight (hr)	Lowest Temp. (°F)
NS-105	TUFF 1	11/14/2021	1.55	-39.34
NS-110	TUFF 1	3/5/2022	1.62	-34.42
NS-111	TUFF DOS	7/31/2022	1.76	-13.71

Table 1. A table of past TUFF flight logistics. “NS” refers to a flight by the BPP Near Space team.

A. Structural Design

One of the key constraints for TUFF DOS was that it be light and small enough to fly above other payloads on any flight. We also created TUFF to be simple enough that other ballooning teams could build copies of TUFF DOS and contribute to a wealth of data with the platform. For a detailed mass and price breakdown of all TUFF DOS components, please refer to *Appendix D*.

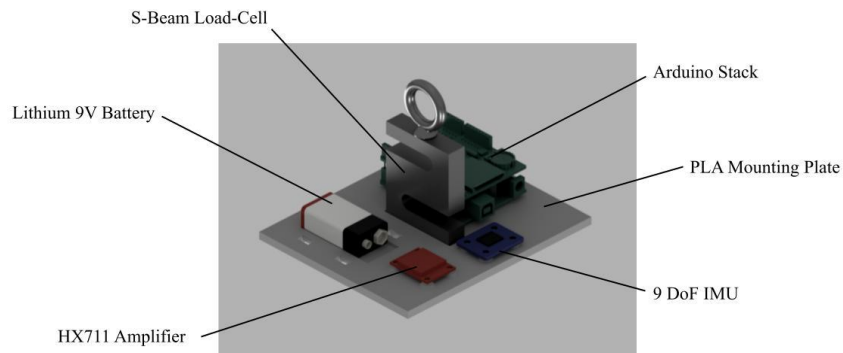


Fig 2. A labeled CAD-rendered image of TUFF DOS internals.

We designed and 3D printed a custom mounting plate for all components within the design to eliminate vibration, internal collisions, and wire detachments mid-flight. The print was created using PLA plastic with 0.2 mm layer thickness to ensure good inter-layer adhesion and at 40% gyroid infill to create a sturdy yet light mounting plate. This printed part is slotted into the top of the foam board box that houses the payload. The eye bolt of the S-beam load cell is screwed into the top of the payload with a washer, through the foam-board and mounting plate into the load cell to secure the load cell and the mounting plate to the foam-board structure. All components are secured to the mounting plate before it is screwed into the foam-board. The load cell is seated in a groove within the mounting plate to eliminate rotation of the load cell relative to the mounting plate during flight, an issue that was identified on the first iteration of TUFF wherein the load cell wires would wrap around the load cell due to its rotation. Most importantly, this design places the entire weight of TUFF DOS onto the top of the load cell so that none of TUFF’s own weight is included in its tension measurement; a partial free body diagram can then be used

to analyze the drag, weight, and tension below the payload, which is expanded upon in *Section III*. Figure 3 is a rendered CAD model of TUFF DOS.

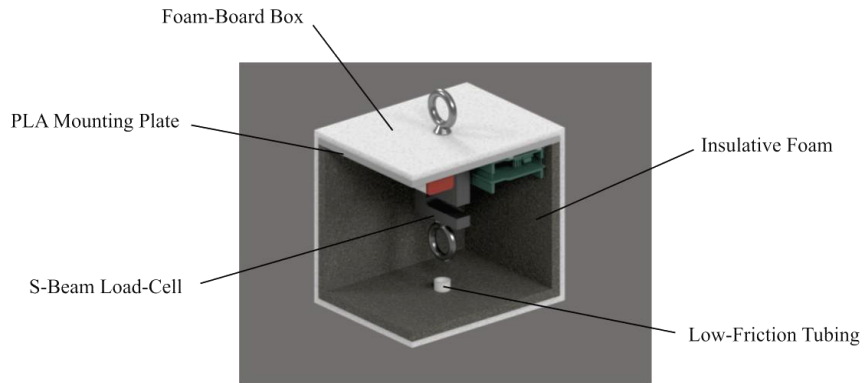


Fig 3. A labeled CAD-rendered section-view image of the assembled TUFF DOS payload.

The cost of TUFF DOS was ~\$300, but the load cell accounts for \$220 of that budget, so anyone interested in replicating TUFF DOS could do so at a greatly reduced cost by purchasing a cheaper load cell. Additionally, the total weight of the payload is 1.4 lbs, which makes it easy to fly TUFF while keeping the total flight train weight below the FAA’s maximum allowable weight of 12 lbs for sounding balloons.

B. Electrical Design

The circuitry in TUFF DOS is relatively simple and has been detailed in the wiring diagram in *Appendix C* for those interested in replicating it exactly. The S-beam strain-gauge load cell from Omega Engineering functions on a standard wheatstone bridge circuit; any load cell with this circuit can operate with the HX711 amplifier that was used in TUFF DOS. Some specifications of the electronics used in TUFF DOS are relevant to the data analysis within this paper, so they are included here. Specifically, the environmental and accuracy ratings of the load cell and BMP280 sensors are listed in *Table 2* and *Table 3* respectively.

Operating Temperature (°F)	Combined Error (%FS)	Safe Overload (%FS)	Ultimate Overload (%FS)
-30 to 140	± 0.02	150	300

Table 2. Relevant ratings for the 25 lb force class C3 S-beam deflection load cell from Omega Engineering, used in TUFF DOS (Full Scale = 25lb).

Operating Temperature (°F)	Accurate Altitude Range (ft from sea-level)	Approx. Abs. Pressure Accuracy (hPa)
-40 to 185	-1,000 to 30,000	± 1

Table 3. Relevant ratings for the BMP280 sensor board, which includes altitude via. pressure and temperature readings. Data above 30,000ft is not used for analysis in this paper, though it is shown in some graphs.

To the extent possible, the TUFF team has limited their data analyses to accurate operational ranges of all involved electronic components. No sensors have been used in potentially damaging conditions, so the integrity and accuracy of all sensors can be trusted. Lastly, based on the power budget located in *Appendix C*, it is worth mentioning that TUFF DOS can operate fully in excess of two hours on a standard lithium 9V battery with minimal concern. TUFF uses a lithium battery as opposed to an alkaline battery to ensure functionality at low temperatures.

C. Instrumentation Methodology

The TUFF team programmed the payload in Arduino C. The code can be found on the GitHub repository in *Appendix A* under the name “TUFFCODECSV.” The code reads sensor measurements, saves them to an SD card in a standard format, and then loops continuously. We take 10 measurements before writing to the SD card for optimization purposes. A high-level block diagram is shown below in *Figure 4*.

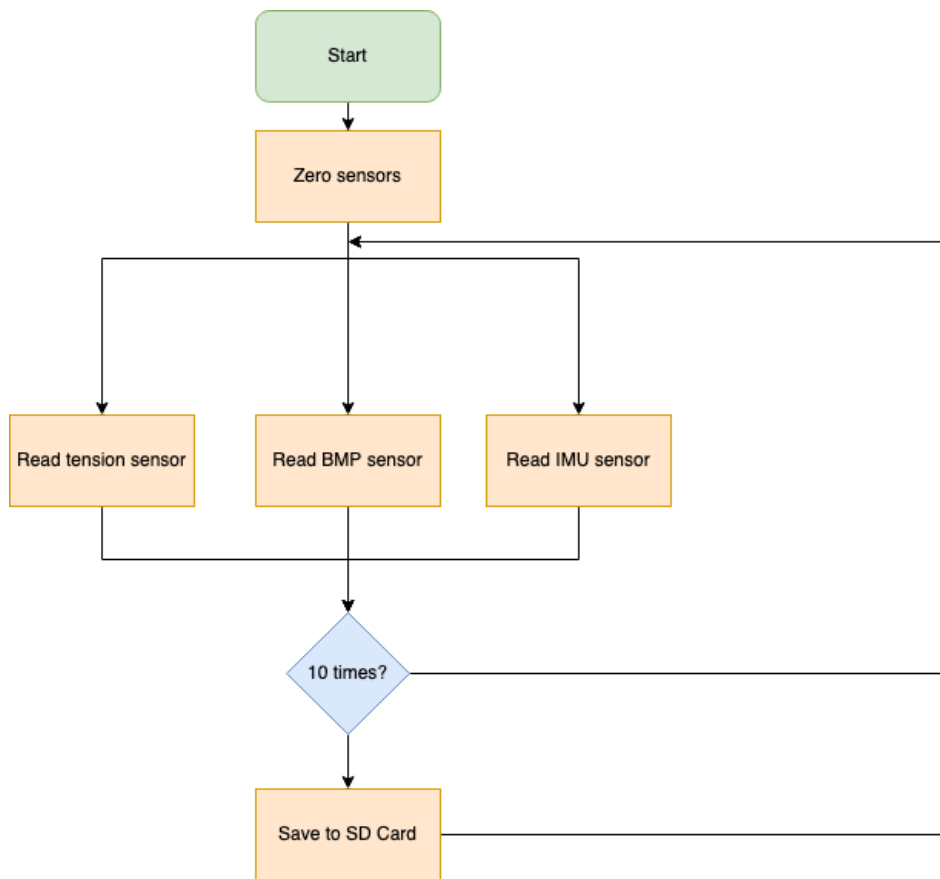


Fig 4. A block diagram showing the in-flight code for TUFF launches.

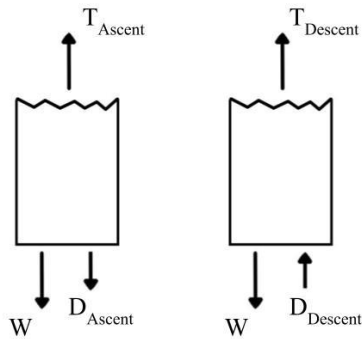
To calibrate our tension sensor, we constructed a test rig and conducted a calibration procedure. The goal was to find a conversion rate between the load cell’s out-of-box units to practical units, in this case pounds. We measured the weight of several calibration masses that were approximately 1 lb using a jewelry scale. At essentially standard sea-level conditions in a lab on UMD campus, we hung the calibration masses from TUFF and recorded its output. To ensure repeatability and to quantify the variability in our measurements, each calibration run consisted of acquiring 10 data points, and the run was replicated 3 times. The calibration dividers from all 3 runs were then averaged to produce the divider that TUFF used in-flight. This value is hard-coded into our in-flight code. We recalibrated TUFF 1 and

TUFF DOS for flights NS-105, NS-110, and NS-111 prior to each flight. The rig for TUFF DOS calibration can be found in *Appendix B*, and the other test rigs were nearly identical. Based on the variability in the calibration data, we were able to calibrate TUFF 1 on NS-105 within $\pm 10\%$, TUFF 1 on NS-110 within $\pm 5\%$, and TUFF DOS on NS-111 within $\pm 3\%$ using this method. This increase in calibration accuracy can be attributed to progressively more accurate scales being used in our process. An example of the experiment and calculations for TUFF DOS can be found in *Appendix B*. These error margins are significantly larger than the rated accuracy of TUFF 1 and TUFF DOS’s load cells, and it is an area the TUFF team hopes to improve for future missions. The calibration code can be found in the GitHub repository linked in *Appendix A*.

The inertial measurement unit (IMU) calibrates itself automatically during setup. The BMP sensor requires a constant for “sea level pressure,” which is assigned before each flight based on weather data. When the TUFF in-flight code begins, all the sensors are zeroed. As such, it is important to keep TUFF still when the code begins to ensure the IMU and load cell are zeroed correctly. Further, for proper zeroing of the load cell, the code must be started while TUFF is lying flat on its side, or while TUFF is hanging on a rope with no weight attached to the bottom. The first method may cause the load cell to measure some of the sensor’s own weight, which may be hard to account for. TUFF 1 on NS-105 and NS-110 was zeroed using the former method, while TUFF DOS was zeroed using the latter method. After the mission ends and the payload is recovered, all sensor data is retrieved from the SD card.

III. Drag

The TUFF payload can be used to calculate drag by finding the difference between the expected tension due to weight and the measured tension, which includes the force of drag while a payload line is in motion. This works both on ascent and descent, though it is important to note that the direction of the drag vector flips with a reversal in the flight train’s direction of movement. The partial free body diagrams in *Figure 5* illustrate how tension and drag relate on both ascent and descent. The drag force seen in *Figure 5* is only the drag experienced by payloads below TUFF on the flightline. It is important to consider the relative placement of partner payloads since TUFF can only provide drag information about the entire collection of payloads below it. To isolate a payload of interest, include the payload at the bottom of a flightline, with TUFF directly above it. TUFF determines the total drag experienced by all items hanging below it using Equation 1.



$$\text{Xa: } |D_{Ascent}| = T_{Ascent} - W$$

$$\text{Xb: } |D_{Descent}| = W - T_{Descent}$$

Note: $T_{Ascent} > W$ and $T_{Descent} < W$ on average in all data used for drag analysis.

Fig 5. Partial Free Body Diagram of TUFF on ascent and descent. **Equation 1.** Drag equations in terms of Tension.

In *Figure 6*, the tension recorded over the duration of flight NS-110 is plotted against time with altitude overlaid. The tension measurements vary since the payload line swings throughout the flight. However, the tension oscillates about a relatively stable average. The nature of these oscillations is discussed further

in *Section IV*. It is important to note here, though, that the fuzzy nature of the tension graph due to variance can disguise certain facts about the data, like its changing average. *Figure 6* also shows average tension values on ascent (9.2lbs) and descent (7.9lbs) in red. One simple explanation of the difference in those averages is the drag changing direction from ascent to descent.

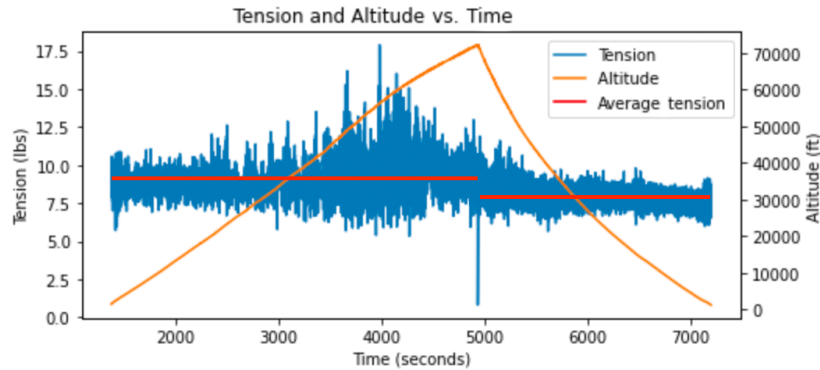


Fig 6. Graph of Tension & Altitude against Time on the NS-110 launch, with added ascent and descent averages to guide analysis.

After application of *Equation 1* to the data in *Figure 6*, *Figure 7* shows the calculated drag of payloads below TUFF 1 on NS-110 over the duration of the flight. Specifically, *Figure 7* shows a rolling average of 1 minute of drag data to simplify any qualitative analysis and present potential trends in the drag experienced by payloads below TUFF. On ascent, drag increases steadily, and on descent, drag also increases steadily after a large drop. These trends appear with varying intensities throughout all three TUFF flights, though their causes are not explored in this paper.

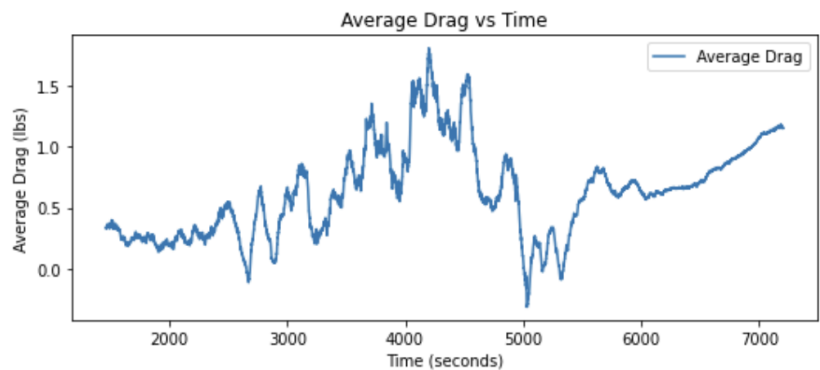


Fig 7. A rolling average of calculated drag over time on NS-110.

To verify the relationship posited in *Equation 1*, the TUFF team used *Equation 3*, which relates calculated drags to velocities squared. Both sides of *Equation 3* should be equal by its derivation from *Equation 2*, as long as the parameters C_d , ρ , and A stay relatively constant throughout the duration of the flight. In order to affirm this assumption, the TUFF team restricted their analysis to the first 10,000ft of ascent and the last 10,000 ft of descent. This carries the added benefit of guaranteeing an upright orientation of the flight train during descent, since the flight train’s parachute is known to take effect in the last 10,000ft of descent. Lastly, one must note that the velocity on ascent and descent is a measured value, though its error is unknown and expected to be inconsequential since TUFF’s measurements of altitude, from which velocity is calculated, have been verified by other payloads.

$$D = C_d \frac{\rho V^2}{2} A$$

Equation 2. Standard drag equation^[5]

$$\frac{|D_{Ascent}|}{|D_{Descent}|} = \frac{V_{Ascent}^2}{V_{Descent}^2}$$

Equation 3. Drag verification test equation

The result of this analysis shows a 1.9% deviation in TUFF’s tension measurement from a perfect equality relationship as prescribed in *Equation 3*, such that TUFF under measured tension. Our calculations can be found in *Appendix B.3*. This result is well within reason considering TUFF’s 5.0% margin of error discussed in *Section II.C*. However, ignoring drag, it is expected that the average tension in the swinging flight train is higher than the weight below TUFF. Ideally, TUFF will have over-measured the tension relative to what we expected by our fixed velocity-squared ratio. However, the 5.0% margin of error in TUFF 1’s tension measurement allows for the proposed relationship, and considerable additional tension, to fall within our error bounds. TUFF DOS was designed to decrease the margin of error down to 0.5% using a new load cell, and account for both the flight train swinging-angle and the flight train orientation on descent using an IMU. However, due to calibration methods and a human error discussed in *Section VI.C*, TUFF DOS drag data is not more accurate than TUFF 1 drag data from NS-110. Future flight data with TUFF DOS will provide more complete analyses of drag properties.

IV. Oscillations

When measuring oscillations within the flight train that are acting on TUFF, it is important to consider the relative placement of partner payloads and their potential influence on TUFF. TUFF is capable of providing information about the oscillations produced by payloads both above and below it. Payloads at the bottom of a flight train might cause pendulum swinging, while payloads higher up might produce standing waves in the flightline.

The TUFF payload can measure oscillations by performing a Fast Fourier Transform (FFT) on the tension data collected by the load cell. As mentioned before, the variation of tension about a stable average value is expected since a payload line swings and gyrates regularly at many frequencies within the same time frame. In order to pinpoint these exact frequencies, the TUFF team extracted 60 second samples from throughout the flight. We took small samples from the flight since oscillation rates change often, possibly with varying wind conditions. The graph in *Figure 8* displays the FFT of a representative 60 second sample.

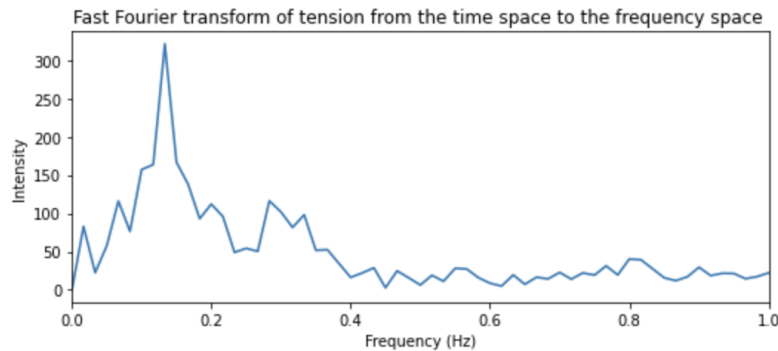


Fig 8. A graph that shows the intensities of different Frequencies (Hz). This graph was generated by FFT. This is a representative 60 second sample from NS-111 at 4,000 seconds after launch. A spike can be seen at 0.135 Hz.

There is a spike at 0.135 Hz, which indicates a 7.4 second oscillation period. This likely means that it took 7.4 seconds for the 6U CubeSat simulator, the heavy payload at the bottom of the flight train on NS-111 pictured in *Figure 1*, to complete each swing in a pendulum motion throughout this 60 second interval. We believe this frequency applies to the 6U CubeSat simulator below TUFF DOS since it is by far the largest influence on TUFF’s tension measurement throughout NS-111. It is a uniquely heavy payload at the bottom of the flight train, so it naturally produces a dominant pendulum swinging motion. Until 5,000 seconds into the flight, we see a range of dominant frequencies in our 60 second samples ranging from 0.125 Hz to 0.185 Hz. We believe that all of these similar frequencies were caused by the 6U CubeSat simulator swinging in different wind conditions. The 5,000 second mark indicates a drastic change in wind conditions, which will be explored later in the paper. For those interested, more Fast Fourier Transform samples can be found in *Appendix A*.

The oscillation rates in a flightline are useful because they give insight into a flight train’s movement at any moment, which can help to understand individual payload flight conditions. Furthermore, the TUFF team suspects that an increase in oscillation rate would cause an increase in TUFF’s tension measurements, so knowledge of the oscillation rate could help account for this. To extend our analysis, we could section our flight into parts and compile a graph of prevalent oscillation rates throughout the entire mission to see how they change over time.

It is important to consider that payload oscillation is rarely a traditional two-dimensional pendulum motion. The payloads tend to move in an oval or saddle-shaped swing, which means there are two simultaneous perpendicular pendulum oscillations. Thus, a single period measurement may not be sufficient to describe all payload pendulum oscillations. Furthermore, the flightline seems to act somewhat like a coupled pendulum rather than a simple one, since there are several masses on the line above and below TUFF. The included IMU in TUFF DOS may help to paint a complete picture of pendulum-related payload flight dynamics in future flights.

V. Shear

Tension measurements can be used to find altitudes with sudden wind-speed changes and turbulence by analyzing the intensity of the tension’s variation about an average. Wind shear is characterized by sudden changes in wind speed and direction; we would expect this to produce increased payload turbulence and swinging, which would increase the variance of TUFF’s measured tension value. This paper calculates the rolling variance of tension across 300 second intervals to quantify tension variation. When measuring variance in TUFF DOS’s tension measurement, it is important to consider its tension sampling rate: TUFF DOS is capable of measuring approximately 40 Hz, meaning that tension variance is fairly accurate even in the context of payload swinging. Below is a graph of tension with a rolling variance function applied.

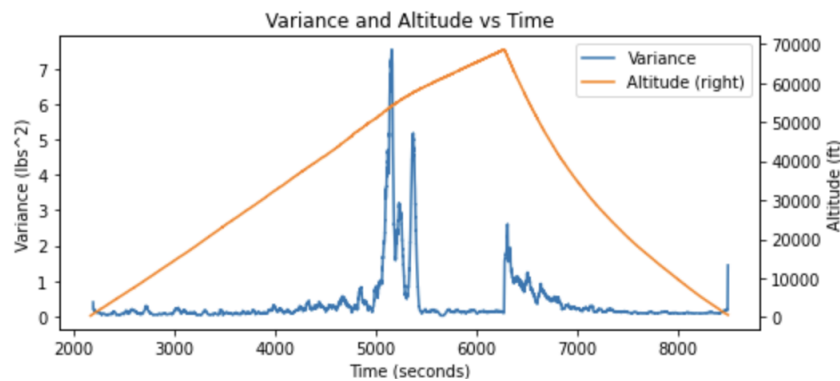


Fig 9. A graph from Matplotlib that shows Rolling Tension Variance (lbs^2) and Altitude (ft) vs Time (seconds). Four clear spikes are seen at 54,100 ft, 57,400 ft, 65,600 ft, and 0 ft in altitude.

The graph shows three significant spikes during the flight, and a fourth spike when the payload lands. The rest of the flight has relatively low variance. The third spike is explained by the balloon popping at the zenith of its flight and initiating free fall. The first two spikes are the largest, and are located at the beginning and end of a region of elevated variance, which we believe indicates high turbulence and wind shear. It is possible that this region represents the effects of the jet stream, as we have seen similar regions of high variance on all three TUFF flights. However, the first spike, which occurred at 54,100 ft, is much higher than the jet stream, as discussed further in *Section VII.C*. The measured increase in variance is confirmed by the oscillation data collected since after roughly 5,000 seconds, the dominant frequency of swinging increases to roughly 0.3 Hz from the 0.135 Hz earlier in the flight. This can be seen in the FFT of a representative 60 second sample in *Figure 10* below.

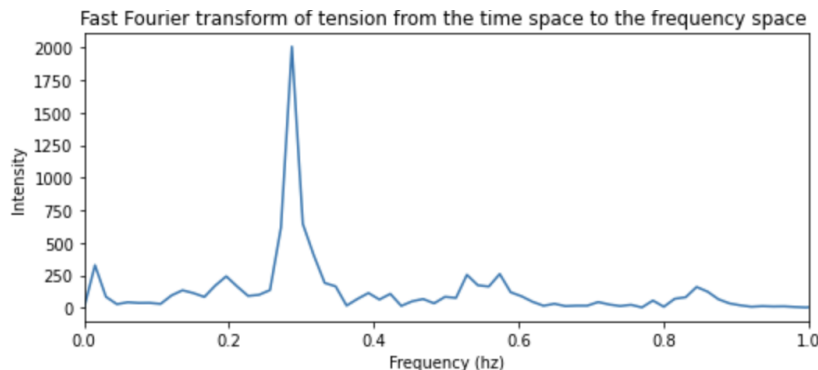


Fig 10. A graph of a fast Fourier transform applied to a 60 second sample of tension data at 5200 seconds. There is a peak at 0.3 Hz.

The importance of atmospheric wind shear data, and potentially jet stream data, in a broader scientific context is mentioned in *Section VII.C*. Here it will be noted that, for ballooning teams that encounter the jet stream or consistent wind shear regularly, it may be helpful to know what effects these atmospheric phenomena typically have on ground tracks, flight speed, and data collection for other missions. To extend our analysis in the future, we will cross-reference the spikes in tension variance with GPS measurements to see whether the balloon’s ground-track speed is affected by detected wind shears as expected.

VI. Challenges and Potential Improvements

As mentioned earlier, the TUFF team sought to verify the calculated drag by testing it against a ratio of velocities squared; this happens to be a small ratio where relatively minute differences in tension can cause large errors. Because of the precise nature of this test, the TUFF team found it very important to identify sources of measurement inaccuracy and come up with effective solutions to reduce error. The TUFF team also had to ensure the safety of all partner-payloads since measuring tension in a flightline requires alterations to the flight train assembly. The ultimate structural failure of TUFF, though highly unlikely, was considered and accounted for. Some improvements to TUFF DOS and our calibration process are planned, and TUFF DOS is scheduled to fly in early October 2022 with solutions to the challenges mentioned in this section.

A. Calibration for Measurement Accuracy

The most important challenge in getting accurate tension readings was the calibration of the load cell. The current solution to this challenge involves the methodology discussed in *Section II.C*. This calibration

gives a value by which all readings must be divided to produce tension measurements in the desired units. However, due to a lack of resources, the calibration process has not been as accurate and consistent as possible. Minor swinging in TUFF has been difficult to eliminate while the payload is hanging. This causes measurement inconsistency by raising the measured tension slightly. Additionally, known weights of higher mass, which would produce a tension of similar magnitude to a flight train, will be used in future calibration. The TUFF team has been using known weights in the range of 100g, and objects whose weights are measured using a scale. The former approach is more ideal when considering the linearity of our load cell, but smaller masses are also more prone to air drafts and swinging in our uncontrolled environment, which will create a high percent error relative to the small measured tension. The latter approach constrains TUFF's accuracy and precision to those of the scale being used.

One solution to the challenge of calibration would be allocating a larger portion of TUFF's funding to the calibration process. Acquiring known weights similar to the weight experienced by TUFF during flights would both streamline the calibration process and reduce sources of error since our calibration would resemble in-flight conditions. This is an important consideration because while light weights can produce inaccuracies during calibration, some heavy weights have also deviated slightly from our load cell's expected linearity during calibration. This could be because our load cell is encountering hysteresis during the loading and unloading process of calibration, most reasonably with the addition and removal of heavier weights. Additionally, a test rig that constrains the swinging of TUFF can be constructed and used to further decrease sources of error.

The issue of zeroing TUFF's load cell relates closely to calibration. Before the flight of TUFF DOS, the team zeroed its load cell while the payload was hanging independently and checked that TUFF was not measuring any of its own weight. For TUFF 1, the team zeroed the load cell under no deflection and measured how much of its own weight TUFF was measuring while hanging. Both approaches are valid, though the TUFF DOS procedure is simpler and reduces the complexity of zeroing for TUFF missions.

B. Flight Safety via Slackline

Another challenge that the TUFF team had to tackle early on was related to the flightline under tension during flight. Normally, in order to measure the tension in a string using a deflection load cell, the line needs to be cut so that the sensor can be placed in between the two ends. However, cutting the line and retying it produced a risk of dropping all the partner payloads below TUFF in the case of structural failure, which was an extreme safety hazard. Since there are other payloads sharing a flight, a failure on the TUFF payload could imperil the whole mission. So, to ensure the integrity of the flight train, a single continuous flightline is optimal. The team came up with a slack-line design, as shown in *Figure 11*, that allowed the flightline to be tied to the TUFF load cell on both ends, with slack in between so as to not break the flightline or interfere with the tension throughout the string. This solution was proven effective on flights and allowed the team to accurately measure the tension of the flightline without cutting it. Although the ultimate failure load of the TUFF DOS load cell is known and safe given the tensions that have been measured, the TUFF team still uses this tie-on method to account for other potential weaknesses in the design, like the eyelet-hooks unscrewing from the load cell under vibration.

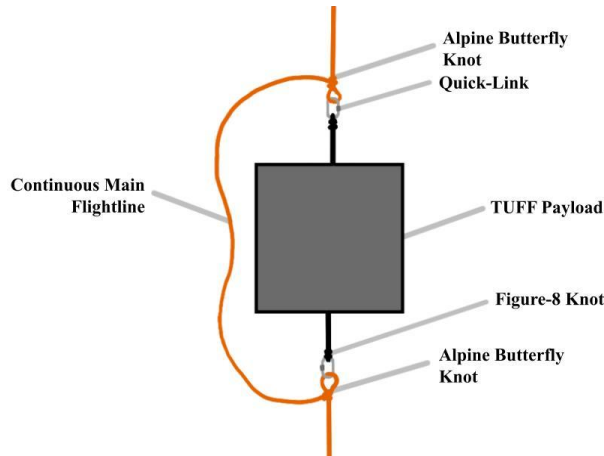


Fig 11. A labeled diagram of the flight line design that enabled the measurement of tension without cutting the flightline.

C. NS-111 Drag Mission Human Error

The TUFF DOS mission on NS-111 was only partially successful. Due to human error during the integration of TUFF DOS into the flight train, the accuracy of the tension data collected post error-correction is a downgrade on NS-110 data. Specifically, a piece of low-friction tubing on the underside of TUFF DOS, which is added to payloads to prevent the flightline from rubbing against a rough surface, was too long and was inserted too far into TUFF DOS such that it contacted the bottom of the load cell. This tube is labeled in *Figure 3*. This removed a portion of the weight experienced by TUFF, since it redirected weight from under the load cell to the TUFF box, which is attached to the top of the load cell. For this reason, NS-111 data is not discussed in this paper within the context of drag measurement despite being excellent in the context of our oscillation and jet-stream missions since it preserves relative tensions. After an attempt at error-correction, the TUFF team found it difficult to measure the exact portion of tension redirected as a result of this mistake. The corrected data is about as accurate as NS-105 TUFF 1 data. Aside from this complication, TUFF DOS has demonstrated a remarkable improvement in accuracy over TUFF 1, and as such is the model described throughout *Section II*. Additional flights for TUFF DOS have been scheduled for the end of 2022 to improve upon previous results and confirm the drag relationship posited earlier in this paper.

VII. Applications

A. Drag

Currently, BPP uses a spreadsheet to calculate the amount of helium necessary to achieve a particular ascent rate on any given flight. This ‘helium calculation’ takes into account many parameters and should consider drag. However, the current models used by BPP for the ‘helium calculation’ do not take into account the drag produced by a flight train, and only consider the drag of the balloon. Furthermore, any drag values used can not be experimentally verified. Depending on the payloads sharing a flight, this unknown variable could cause inaccuracy when targeting an ascent rate. Including the flight train’s drag could allow BPP and other ballooning teams to more precisely fill their balloons for desired ascent rates.

The measurement of drag via the TUFF system can be applied to any advanced payload as a supplement to the typical testing done on a balloon platform. Some research teams have demonstrated interest in measuring drag on uniquely shaped balloon payloads^{[1][2]}. More clever applications of live tension

measurements at larger scales can provide details about aerodynamic flow on planes and the lift forces produced by it. The general concept behind TUFF's application may merit consideration for aerospace systems that benefit from live measurements or which are impractical to test in a wind-tunnel.

B. Oscillations

Currently, the most common methods for acquiring insight into how a flight train swings throughout a flight are video recordings captured by payloads and IMU data^[2]. Any payload seeking to mitigate this swinging or take stabilized video despite this swinging would need detailed quantitative data about the motion it will encounter, which requires more precision than can be extracted using these methods. The many coexisting oscillation frequencies produced by many masses on a long string as it travels through the atmosphere are too difficult to discern with a dedicated IMU, or even a set of IMU payloads. TUFF has the unique ability to quantify the consistent oscillating motion in a flight train throughout an entire flight using a single sensor placed anywhere on the flightline. This includes the pendulum swinging of the flight train, along with any standing waves, which are especially hard to quantify. There is also a potential to develop a general model for the motion of spread masses along a swinging line using TUFF data across many flights.

C. Shear Winds

For those interested in the effects of wind shear on their flight train, TUFF's empirical data may prove to be most convenient and relevant as opposed to large-scale atmospheric models. It is possible that high-speed winds within the upper-atmosphere may drastically increase or decrease the speed of a balloon's travel as it passes through them. Such unexpected changes may cause a flight to deviate from ground-track predictions. More information about the future path of a balloon, through knowledge of its likely deviations, can aid in establishing line of sight communications, avoiding restricted airspace, and planning recovery missions.

It is possible that the two major spikes in tension variance measured by TUFF are related to the boundaries of the local jet stream. Since BPP launches from Maryland, we are primarily concerned with the subtropical jet stream. Interestingly, this jet stream is known to exist from 32,800 ft to 49,200 ft^[4], yet our results show elevated tension variance from 54,100 ft to 57,400 ft, indicating that, barring altimeter errors or a vertical displacement of the jet stream, the jet stream winds themselves are not what is directly increasing tension variance. We note that the smaller range of increased variance, relative to the usual height of the jet stream, does not exclude these altitudes from indicating jet stream boundaries, as TUFF could have taken the path of a secant through the jet stream, intersecting it only briefly.

Though there is scientific discussion surrounding the jet stream's movement poleward (North) as a result of climate change, little attention has been given to its altitude and whether or not it is changing^[6]. Some researchers even claim that the higher altitudes considered within jet stream study methodologies cause disagreements between competing models^[6]. There is no overall scientific consensus on the movement of the jet stream, and our unusually high altitude measurements may be explained by other phenomena. However, TUFF may be able to contribute to this area of atmospheric science research considering the state of discussion. More research is required to discern whether TUFF's increased variance regions are in any way a result of the jet stream or related atmospheric phenomena.

Lastly, if multiple TUFF DOS payloads are built, with each one harvesting data across a geographic area, a live model of local wind shears, and potentially jet stream-related altitudes, could be developed. In either case, TUFF's data may be useful for studying the effects of climate change on the local atmosphere across different geographic regions.

VIII. Conclusions

The data we have collected so far suggests that the tension measurement capabilities of TUFF DOS can be developed and eventually used to optimize high-altitude balloon missions. Specifically, the TUFF platform has shown a convincing capability to calculate drag, oscillations, and wind shear altitudes. Furthermore, the capabilities of tension measuring devices seem uniquely capable of providing this data on balloon missions. This data in turn can improve the efficiency and accuracy of balloon mission operations. The TUFF team will continue to address challenges on future flights and in future design iterations. We will also reach out to atmospheric modeling specialists regarding jet stream data to develop a case for, or against, the jet stream measurement utility of TUFF. The most important goal of this project going forward will be to decrease measurement error and increase the number of variables accounted for in a swinging flightline, which could lead to a simulated model of balloon flight dynamics.

Readers are encouraged to replicate the TUFF experiment on their own high-altitude balloon mission, and the TUFF team welcomes the sharing of data regarding TUFF-like measurement systems. All TUFF data is continually posted on the BPP data archive, which can be found at <https://bpp.umd.edu/archives/>.

IX. References

- [1] Flaten, J. & Gosch, C. & Habeck, J. (., (2015) “Techniques for Payload Stabilization for Improved Photography During Stratospheric Balloon Flights”, *Academic High Altitude Conference 2015*(1). doi: <https://doi.org/10.31274/ahac.5570>
- [2] Gemignani, M.; Marcuccio, S. Dynamic Characterization of a High-Altitude Balloon during a Flight Campaign for the Detection of ISM Radio Background in the Stratosphere. *Aerospace* 2021, 8, 21. <https://doi.org/10.3390/aerospace8010021>
- [3] Mudd, M., (2022) “Active Stabilization for Imaging Devices”, *Academic High Altitude Conference 2020*(1). doi: <https://doi.org/10.31274/ahac.11643>
- [4] Luna-Niño, R., Cavazos, T., Torres-Alavez, J.A. *et al.* Interannual variability of the boreal winter subtropical jet stream and teleconnections over the CORDEX-CAM domain during 1980–2010. *Clim Dyn* **57**, 1571–1594 (2021). <https://doi.org/10.1007/s00382-020-05509-7>
- [5] “The Drag Equation.” NASA, NASA, <https://www.grc.nasa.gov/www/k-12/airplane/drageq.html>.
- [6] Woollings, Tim, and Mike Blackburn. "The North Atlantic Jet Stream under Climate Change and Its Relation to the NAO and EA Patterns". *Journal of Climate* 25.3 (2012): 886-902. <<https://doi.org/10.1175/JCLI-D-11-00087.1>>. Web. 15 Sep. 2022.

X. Acknowledgements and Appendices

The Maryland Space Grant Consortium (MDSGC) generously funds the operations of the University of Maryland College Park’s Balloon Payload Program. This club provides unique opportunities for undergraduate and graduate-level students to design and fly scientific payloads on high-altitude weather balloons. BPP has completed over 100 launches since its creation in 2003 by Dr. Mary Bowden. Without Dr. Bowden and the MDSGC, this paper would not have been possible.

Dr. Thomas Snitch has also been instrumental in the development of TUFF DOS. We are grateful for the funding he provided us, which allowed for the purchase of the TUFF DOS high-accuracy load cell.

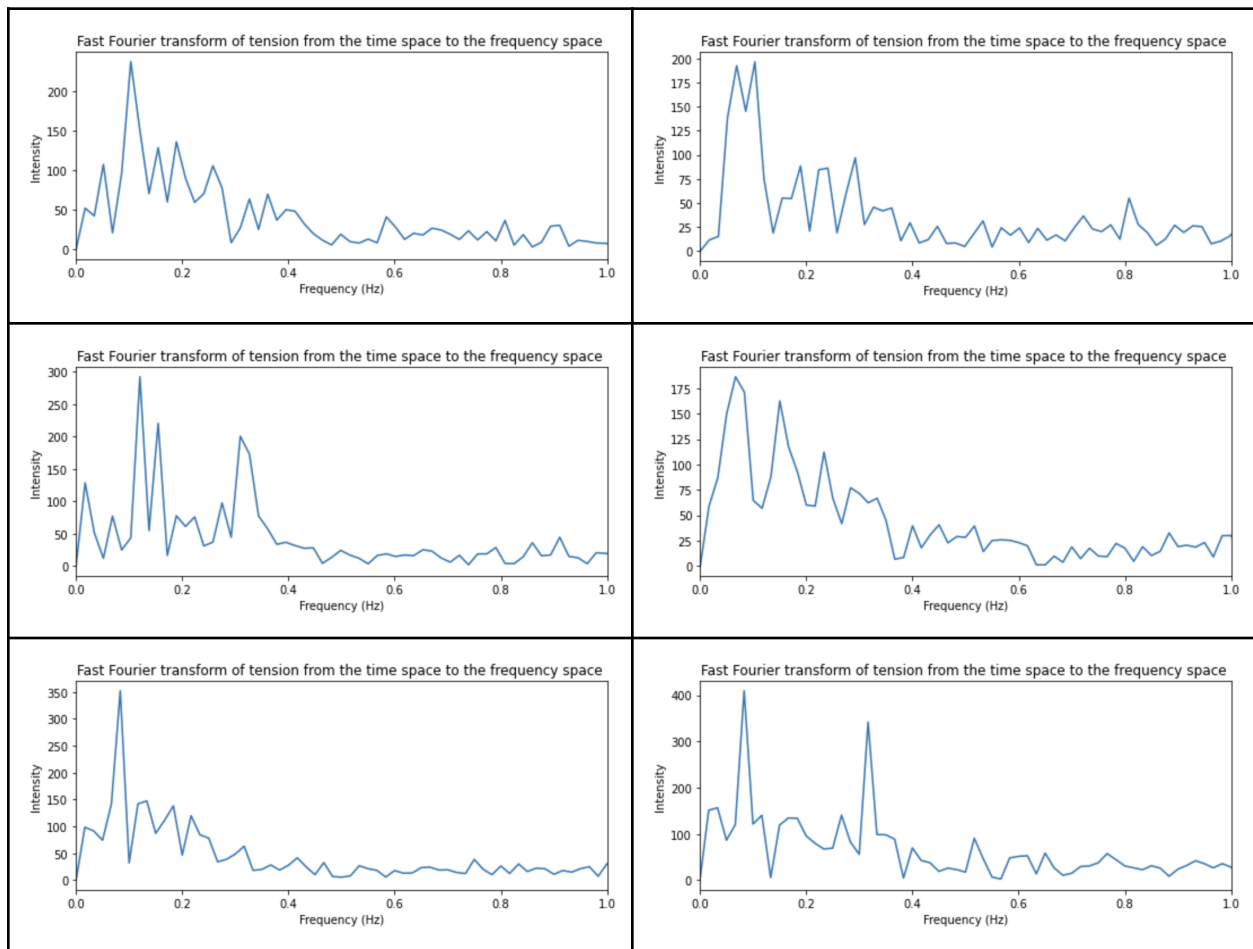
We would like to thank Dr. Alison Flatau, the University of Maryland College Park Aerospace engineering department chair, for helping us edit our paper and for helping us properly communicate our results to an academic audience.

Lastly, we want to express gratitude to all of our peers in BPP at the University of Maryland, College Park. Their advice and support has helped to build this project from the ground up. Special thanks are owed to Madeleine Lebetkin and Alexis Burris for mentoring the TUFF team in its infancy.

Appendix A - Programming Resources

<https://github.com/Gidntsquia/TUFFcode>

Fig A.1. Github repository of payload code and analysis code.



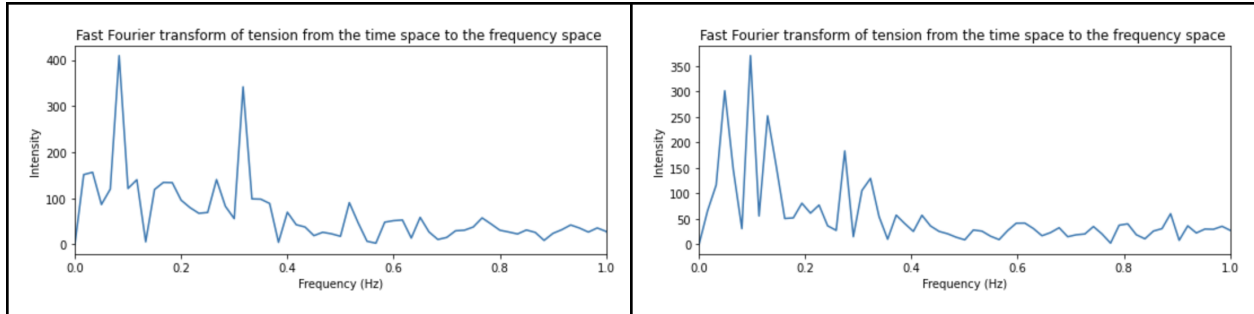


Fig A.2. Eight Fast Fourier transform graphs every 100 seconds starting from 3700 seconds to 4500 seconds, excluding 4000 seconds, which is already shown in *Figure 8*.

Appendix B - Calculation Resources

<https://docs.google.com/spreadsheets/d/187oAItUjHugEfo0IwhCXrhoz8yT0nBRF83yqK8HZTfo/edit#gid=0>

Fig B.1. Google Spreadsheet outlining our tension sensor calibration procedure and results.



Fig B.2. Photograph of TUFF DOS calibration test rig. 500 g jewelry scale used along with various objects around the lab weighing under 500 g each, totaling roughly 15 lbs in total.

<https://docs.google.com/spreadsheets/d/12MzcHWLXqzLgLZ56cs3OEGbjPwLi2tpHEkvx9II1uc/edit#gid=0>

Fig B.3. Google Spreadsheet outlining our drag measurement verification calculations.

Appendix C - Electronics Resources

Component Name	Amount of Component	Operating Voltage (V)	Supply Current (A)	Operating Time (hrs)	Ah
Arduino UNO	1	5	0.05	1.5	0.08
RTC	1	5	0.00	1.5	0.00
HX711 (Amplifier)	1	5	0.002	1.5	0.00
SD Card Writer	1	5	0.04	1.5	0.06
BMP280	1	5	0.00	1.5	0.00
9-Axis IMU	1	5	0.01	1.5	0.02
load cell	1	Power draw included in HX711's operation.			
Total:					0.16

Table C.1. A power budget including all of TUFF DOS's electrical components.

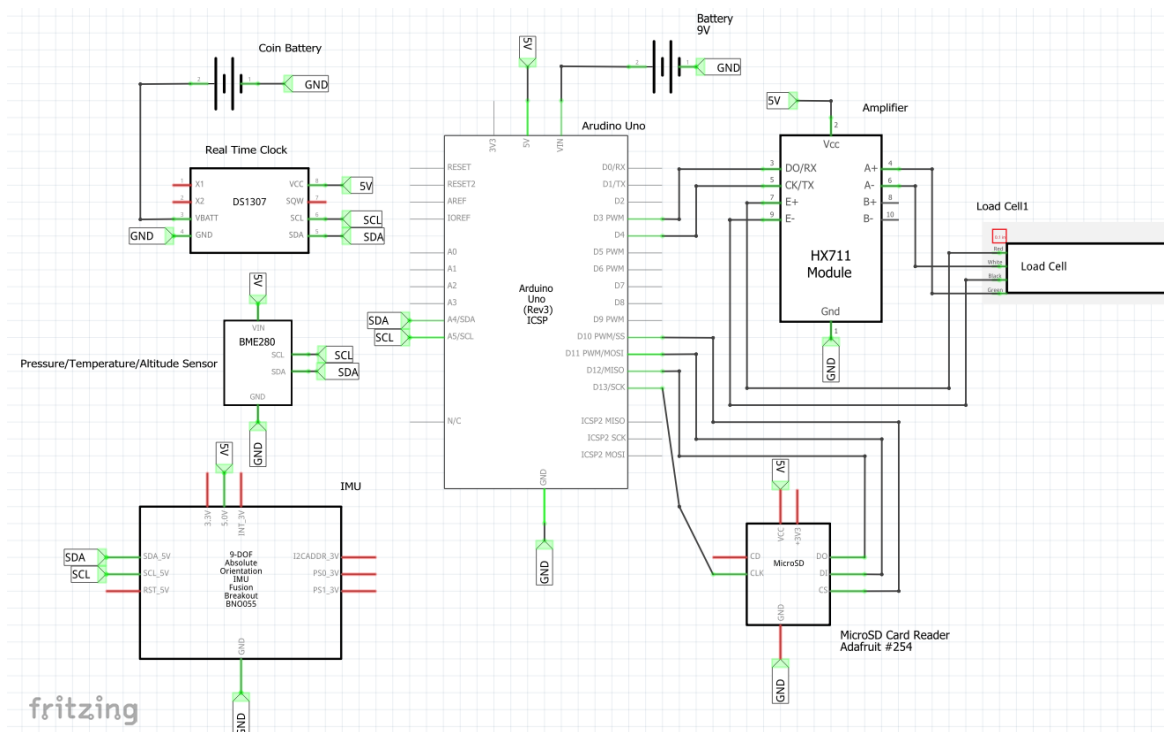


Fig C.2. Wiring diagram of TUFF DOS circuitry.

Appendix D - Components List and Mass Budget

Component Name	Amount of Component	Mass (g)	Price (USD)
Arduino UNO	1	25	27.60
RTC	1	1.2	6.95
HX711 (Amplifier)	1	1.5	10.95
SD Card Writer	1	4.3	7.50
BMP280	1	1.3	9.95
Lithium 9-Volt Battery	1	36	12.97
load cell	1	230	210
Mounting Plate (PLA)	1	75	negligible
Eye Bolts	2	28	6.28
	Total:	430	298.48

Table D.1. Mass and price breakdown for TUFF DOS components. Foam-board and insulation are not priced or weighed in the above table.